FOOT PLACEMENT CONTROL UNDERLIES STABLE LOCOMOTION ACROSS SPECIES

Antoine De Comite[1] and Nidhi Seethapathi[1,2,3,*]

[1]McGovern Institute for Brain Research, MIT, Cambridge MA 02139, USA
[2]Department of Brain and Cognitive Sciences, MIT, Cambridge MA 02139, USA
[3]Department of Electrical Engineering and Computer Science, MIT, Cambridge MA 02139, USA
[*]Correspondence should be addressed to N. Seethapathi: nidhise@mit.edu

ABSTRACT

Animals navigate their environment stably without inefficient course corrections despite unavoidable errors. In humans and some robots, this stability is achieved by controlling the placement of the foot on the ground such that recent movement errors are corrected. However, it is unknown whether and how animals with diverse nervous systems and body mechanics use such foot placement control: foot trajectories of many-legged animals are considered as stereotypical velocity-driven patterns, as opposed to error-driven. Here, we posit a control structure for stabilizing foot placement in any legged embodiment by unifying velocity-driven and body state-driven contributions, and develop a framework to discover control strategies used across species from natural locomotor variability. Using this framework, we find evidence for body state-dependent foot placement control in flies and mice, previously only shown to exist in humans. We discover that the urgency and centralization of the foot placement control strategy is shaped by the animal's neuromechanical embodiment. More inherently stable many-legged embodiment is associated with a lower control magnitude and timescale. Further, many-legged embodiment is accompanied by decentralized control with modular control functions, timescales, and gains, whereas analogous functions are centralized across both legs in humans. Our approach discovers signatures of stabilizing control across species and reveals how different neuromechanical embodiments achieve a shared functional goal: foot placement control.

Introduction

Legged locomotion is a fundamental motor skill for navigating complex everyday environments. The ability to move stably from place to place in the presence of time-varying sensorimotor errors is a crucial component of locomotion; unstable locomotion can result in time-consuming course corrections or injury-causing impacts on the body [73, 87]. In human and robot locomotion alike, control of the swinging leg in a manner that corrects perturbations to the body has emerged as an important strategy for stability [89, 13], termed 'foot placement control'. However, we do not understand whether and how this important function is achieved across species with different brains and bodies, i.e. across *neuromechanical embodiment*. Indeed, in many-legged animals the actuation and coordination of the limbs is thought to be largely top-down and velocity-dependent [47, 37]. Here, we posit a control structure underlying stable locomotion in any legged embodiment, unifying velocity-dependent 'feedforward' and body state-dependent 'feedback' contributions to foot placement. Based on this hypothesized controller, we develop a data-driven framework to infer signatures of control from high-throughput locomotion data. We discover signatures of body state-dependent foot placement control hidden in natural locomotor variability in flies (*Drosophila melanogaster*), mice, and humans, previously only known to exist in humans on treadmills [89]. We find that key functional aspects of the control are conserved across these two-, four-, and six-legged species and characterize the control strategy used: the input space, gains, timescales, and centralization of the control. Our findings help understand how species with different neuromechanical embodiments achieve a shared functional goal: stable locomotion by foot placement control.

Foot placement control i.e. placement of the swinging leg in a manner that counters perturbations, is an important contributor to dynamic stability in bipedal locomotion [13]. Work in the 1980s on building dynamically stable hopping robots [73, 72] and mathematical models of bipedal walking [87] foreshadowed the importance of foot placement control. Later, empirical work found that the structure of human locomotor variability is consistent with active feedback control of foot placement [6, 44]. A theoretical control rule posited that foot placement in the next step should be informed by body state errors in the current step [43], and subsequent data-driven work showed that humans indeed employ this control strategy when walking on a treadmill [89]. This rapid transformation from body-related information into corrective foot placement can rely on visual [59, 3], proprioceptive [20, 75], and vestibular [8, 29] sensory feedback, recruiting spinal [34] and supraspinal [38, 83] nervous centers. This makes foot placement control vulnerable to neuromotor disorders, and indeed has been found to be impaired in some patient populations [63, 48, 64, 91, 52]. Identifying common signatures of stabilizing foot placement control across species with different bodies and brains would provide insight into its neuromechanical basis. Here, we put forth a data-driven framework that generalizes across species, and find that mice and flies use foot placement control for stable locomotion, previously only shown in humans.

Neural control of locomotion is thought to have both feedforward and feedback contributions [54]; feedforward control is task-dependent and not informed by continuous sensory feedback, whereas feedback control is informed by multi-modal sensory information. Feedforward control of locomotion by pattern-generating neural networks [18, 47] governs the stereotypical inter-limb coordination patterns across species [41, 40, 42, 7, 16, 9, 67, 57]. These pattern-generating networks interact with reflexive feedback loops [27], integrating information from somatosensory, vestibular, and visual sources. However, the nature of this feedforward-feedback interaction and its role in locomotor stability is poorly understood [1, 46]. While our understanding of central pattern-generating circuits has benefited from behavioral measures of the periodic inter-limb coordination [76, 35], we lack analogous behavioral measures to understand the feedforward-feedback control underlying locomotion [88, 77, 93, 2]. Here, we put forth a data-driven framework that quantifies the feedforward velocity-dependent and feedback body state-dependent contributions to foot placement control across species.

In addition to the nervous system, locomotor control is shaped by the species-specific mechanical properties of the body [68, 46], and therefore vary across embodiment. Passive biomechanical properties such as the body's size, weight, inertia, stiffness, and damping can shape both feedforward and feedback control of locomotion. The maximum running speed achieved by an animal varies across species [33] and is explained by the differences in body mass and the muscle properties [55]. Different neural transmission delays and reaction times across species can be explained by differences in their size and inertia [62, 61, 84]. The number of legs simultaneous in contact with the ground during locomotion provides passive lateral stability [81]. Investigating feedforward-feedback locomotor control in diverse species will help understand how different brains and bodies co-evolved to achieve a shared functional goal. We provide a cross-species generalizable framework to investigate how stabilizing control strategies are shaped by the animal's embodiment.

In this study, we investigate foot placement control strategies for stable locomotion across species with diverse neuromechanical embodiment. Our approach and findings have implications for comparative neuroscience, evolutionary biomechanics, and legged robotics. We discover aspects of foot placement control that are shared between humans and neuroscientifically accessible animal models like flies and mice. These findings improve our ability to transfer insights about the neural basis of stable locomotion across species [31], and to investigate animal models of instability-inducing disorders in humans [1]. Our data-driven framework is generalizable across legged species and provides a starting point to understand how diverse nervous systems and body mechanics co-evolved to achieve stable locomotion on evolutionary timescales [45]. Understanding how different neuromechanical embodiments achieve the common functional goal of dynamic stability, as we do here, can help identify cross-embodiment principles [95] for designing and controlling legged robots [82].

Results

We hypothesize a feedforward-feedback foot placement control structure for stable locomotion in any legged animal, and discover signatures of the hypothesized control hidden in natural locomotor variability. We characterize these control strategies in flies (*Drosophila melanogaster*), mice (C57BL/6J), and humans using high-throughput locomotion data. We discover that these strategies vary systematically across species; showing how timescales, control gains, body state-dependence, and centralization change across species.

Hypothesized feedforward-feedback structure underlying foot placement control

We posit a hierarchical feedforward-feedback control structure underlying stable locomotion in any legged species. Our control structure consists of a feedforward module (Figure 1A, red) that generates a *nominal* trajectory based

on velocity and heading inputs, and a feedback module (Figure 1A, blue) that makes corrective adjustments to the foot placement based on errors in the body state with respect to the nominal. We rationalize the feedforward module by animal neuroscience research [32, 94, 14] suggesting that velocity and heading are important descending inputs for the generation of periodic inter-limb coordination patterns. We rationalize the feedback module by human locomotor stability research on body state error-based modulation of foot placement in healthy [43, 89] and disordered [63, 48, 64, 91, 52] locomotion. Our hypothesized feedforward-feedback control structure is hierarchical as it contains privileged inputs at each module; the feedforward module has access to the desired velocity and heading but not the body state errors, while the feedback module has access to the body state errors but not the desired velocity. The hypothesized control structure is also multi-timescale, the feedforward module operates at a slower timescale of the order of multiple steps, while the feedback module operates on a faster timescale (Figure 1A).

The feedforward and feedback modules have differing inputs, but control the same motor output: foot placement. The feedforward module outputs the nominal foot placement according to the canonical gait patterns adopted by each species (Figure 1B). The intrinsic sensorimotor noise, putatively due to neural, sensory, or muscular sources, necessitates a feedback controller; in the absence of such feedback controller, the animal would exhibit uncontrolled drift (Figure 1C). The feedback control module takes in the deviations from the nominal body states to make corrective modulations of the foot placement. If this hypothesized control structure underlies foot placement control, we should find velocity-based and body state error-based contributions to behaviorally observed foot placement (Figure 1D). In the following sections, we provide evidence for such statistical signatures of the hypothesized feedforward and feedback contributions to foot placement control in locomotor variability in flies, mice, and humans.

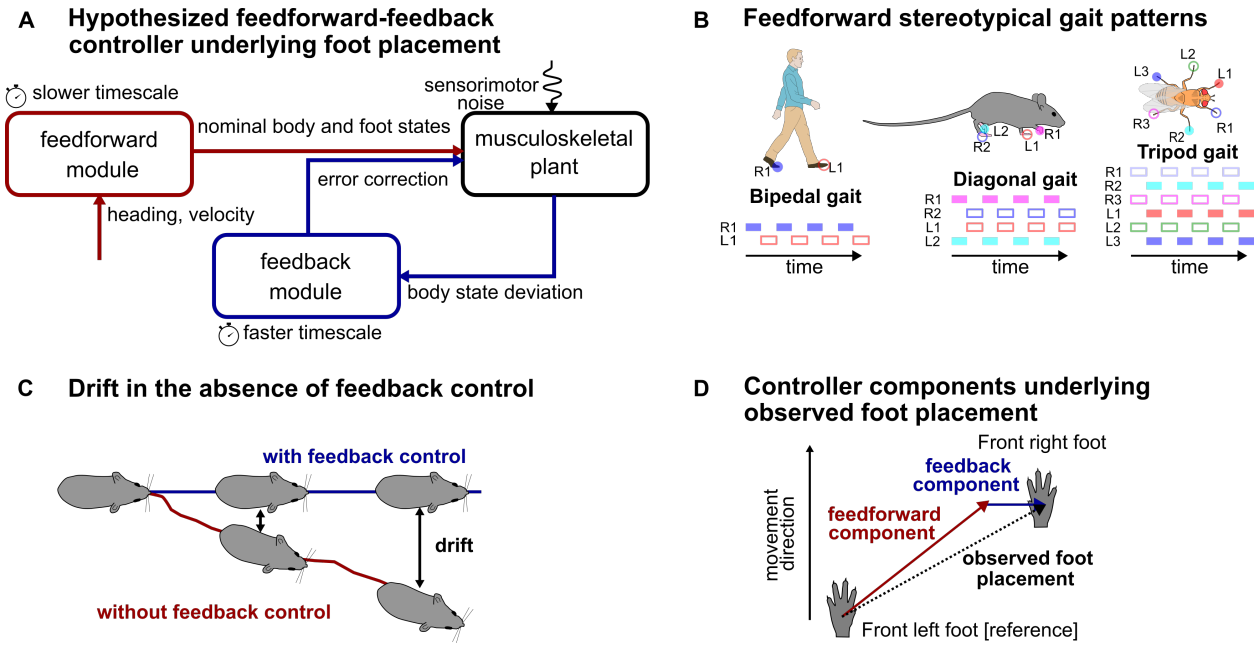

Figure 1: Hypothesized feedforward-feedback control structure for stable locomotion in legged animals. **A** Schematic representation of interactions between the velocity-dependent feedforward control module (red) and the body state-dependent feedback control module (blue). The feedforward module transforms descending inputs into nominal foot placements for multiple gait cycles. The feedback module corrects body state errors by making appropriate changes to the foot placement. **B** Canonical gait patterns for humans, mice and flies. The colored rectangles indicate the times at which each limb is in stance, while full and empty rectangles illustrate the two groups of legs alternatively in contact with the ground during the canonical gait pattern as illustrated by the colored circles on the animal's body. **C** Positional drift due to intrinsic sensorimotor noise in presence (blue) and absence (red) of feedback control. **D** Observed foot placement as the sum of feedforward and feedback components. The feedforward module controls the nominal foot placement (red) and the feedback control module (blue) applies corrective modulations to this nominal foot placement.

Signatures of velocity-dependent feedforward foot placement across species

Our feedforward-feedback control structure (Figure 1A) posits that movement velocity contributes to the foot placement control adopted by the animal. While the contribution of movement velocity to foot placement variability has been characterized in humans [19], this relationship less understood in other species. To simultaneously test our hypothesized

feedforward module and understand the nature of its velocity-dependence in many-legged animals, we took a data-driven approach; we correlated the movement velocity with the nominal foot placement to understand which aspects of foot placement are informed by the movement velocity. We calculated the nominal lateral position i.e. step width and the nominal fore-aft position i.e. the step length of each foot relative to the reference foot (Figure 2A).

We found that movement velocity modulated the step length but not the step width across all limbs and all species. Flies increased their step lengths with increasing movement velocity (8/8 videos significant for front, central and hind limbs, Figure 2D top blue, green and magenta respectively) while their step widths remained unaltered (0/8 videos significant for all limbs, Figure 2D bottom). Similar behavior was observed in mice where the step lengths were modulated with movement velocity for both front (79/80 subjects significant, Figure 2C, magenta top) and hind limbs (44/80 subjects significant, Figure 2C cyan top), while their step widths were unaltered by the velocity for both front (18/80 significant, Figure 2C magenta bottom) and hind limbs (18/80 subjects significant, Figure 2C cyan bottom). Humans increased their step lengths with increasing movement velocity (20/21 subjects significant, Figure 2B top), while their step widths were unaltered by the velocity (1/21 subjects significant, Figure 2B bottom).

Thus, we found that the impact of the movement velocity is similar across all species and limb pairs, and modulates the nominal foot placement as hypothesized. We find that this dependence on velocity impacts the fore-aft nominal foot placement i.e. the step length and not the step width in all species. Faster movement velocities give rise to longer steps and do not significantly alter the step width.

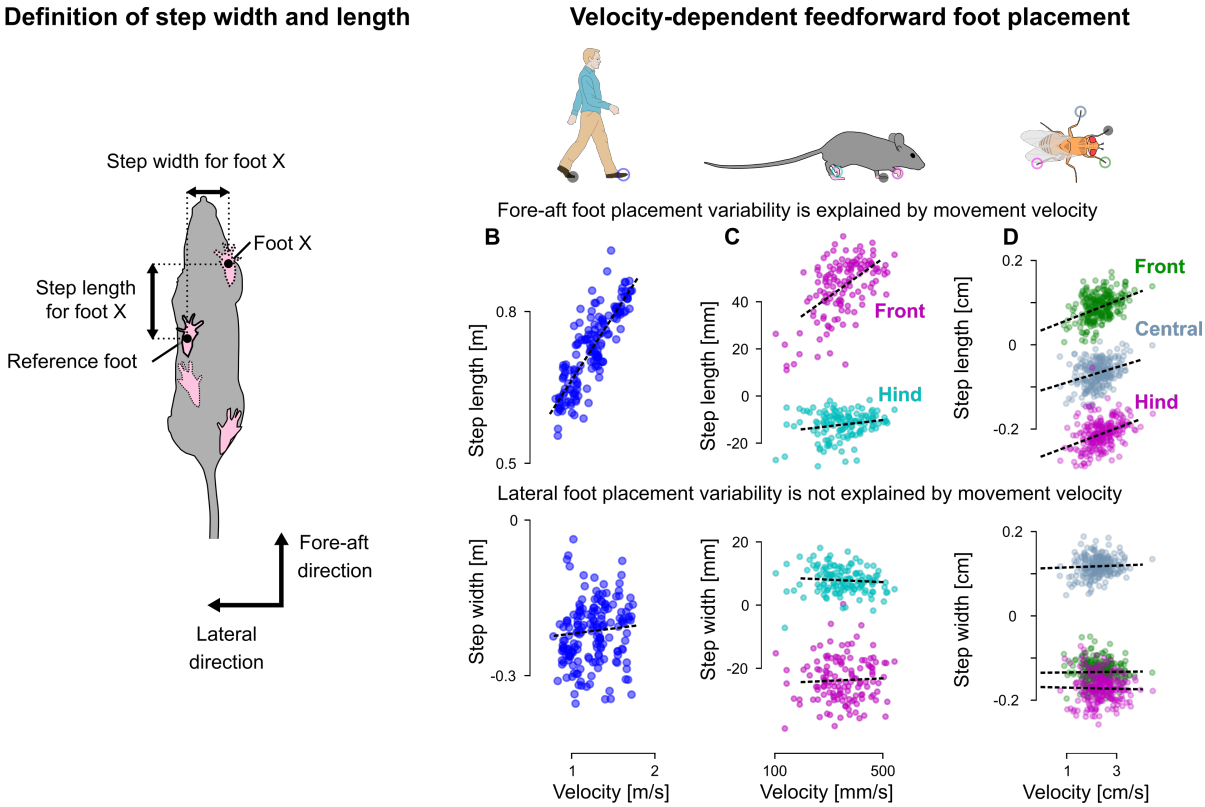

Figure 2: Signatures of velocity-dependent feedforward foot placement control. **A** Bottom view of a mouse walking. The feet outlined by full and dashed contours respectively represent the feet in stance and swing (i.e, the foot about to be placed). The step width and length are defined as the distances along the lateral and fore-aft directions, respectively, between the reference foot and the contact foot to be placed. **B-C-D** Modulation of the step length (top row) and step width (bottom row) as a function of the fore-aft movement velocity for individual limbs in humans, mice (front - magenta, hind - cyan) and flies (front - green, central - blue, hind - magenta), representative data. The black dashed lines capture the individual regressions between movement velocity and the step width/length. The reference limbs with respect to which the step width and length are defined for each species are represented by the transparent black disk overlaid on the illustration of the animals, the open disks represent the different contact feet.

Signatures of body state-dependent feedback foot placement across species

Our hypothesized feedback module (Figure 1A, blue) posits that the errors in the body state occurring on each step should inform the future foot placement variability exhibited by the animal. Here, we test this hypothesis and characterize the feedback control module by identifying a mapping between the body state errors and the future foot placement, quantifying the variance explained by this mapping as a function of gait fraction. Such a mapping between body state errors and foot placement variability has previously been discovered in human treadmill locomotion [89, 74, 80], but its existence is unknown in other legged species and for natural overground locomotion in humans. To characterize this mapping in many-legged species, we calculated the errors in the body state and foot placement as a function of gait fractions (Figure 3A), and identified linear mappings relative to the respective nominal values (see *Methods*). We then compared these mappings to a baseline one based on the foot kinematics alone, to understand whether the body state errors contain more information about future foot placement than the trajectory of the foot itself. If the body state informed the future foot placement, as suggested by our hypothesized feedback control module (Figure 1A, blue), the body state information should be predict the eventual foot placement before the beginning of the swing phase of the contact foot to be placed (see Figure 3A for the definition of the beginning of the swing phase).

We found that body state errors predicted future lateral foot placement in the front limbs of flies, mice, and humans. Moreover, in all species the body state errors predicted future foot placement variability in advance of the foot trajectory predicting itself. In flies, the body state-based predictions outperformed the baseline from the beginning to up to 65% of the gait cycle (two samples Kolmogorov-Smirnov test ($p<0.05$), Figure 3B, right), while the swing phase of the contact foot began around 55% of the gait cycle. In mice, the body state-based predictions outperformed the baseline predictions from the beginning to up to 70% of the gait cycle (two samples Kolmogorov-Smirnov test ($p<0.05$), Figure 3B center), while the swing phase of the contact foot began around 50% of the gait cycle. In humans, the body state-based predictions outperformed the baseline predictions from about 30% to 80% of the gait cycle (two samples Kolmogorov-Smirnov test ($p<0.005$), Figure 3B left), while the swing phase of the contact foot began around 65% of the gait cycle. In all three species, we observed that the predicted deviations by the body state-based model (Figure 3C top blue, exemplar data) were more accurate than the predictions made by the baseline model (Figure 3C bottom red, exemplar data) well before the initiation of the swing phase.

Thus, we found that the lateral foot placement of the front limbs in mice and flies can be predicted by the body state-dependent errors before the initiation of the swing phase of the contact foot at timescales shorter than the sensorimotor delays measured during locomotion in these species [61], similar to humans. These findings suggest the existence of a body state-based foot placement controller in the lateral direction during natural locomotion across species.

Signatures of control magnitude and timescale vary across embodiment

We have found a qualitatively similar body state-dependent foot placement control strategy in the lateral direction, hidden in locomotor variability, in flies, mice, and humans. However, the details of the control strategy – such as how much error is corrected and over what timescale – may vary across species due to more passively stable embodiment afforded by multiple limbs. To understand how the amount of error corrected in each step, namely the *control magnitude*, varies with embodiment we computed the maximal difference between the coefficient of determination of the body state error-based model relative to the foot trajectory-based baseline model (Figure 4A insert) for each individual regression, and compared it across species. We observed a gradient across species (Figure 4A) with the largest differences observed in humans (0.61 ± 0.14), followed by mice (0.31 ± 0.12) and by flies (0.14 ± 0.04). These results suggested that, although these species leveraged qualitatively similar body state-dependent foot placement control strategies, the extent to which errors are corrected in a single step vary with many-legged embodiment. Specifically, the explained variance by body state error-based control decreased with increasing passively stable embodiment.

While we found that the body state-dependent foot placement control magnitude was lower for more passively stable animals, this did not tell us about the *control timescale* i.e. over how many foot contacts the error was corrected. To capture that control timescale, we computed the correlations between a given lateral foot placement of a limb and its subsequent lateral foot placements (Figure 4B). These correlations, captured by the Pearson coefficient, exponentially decayed with time (Figure 4C, illustrative data). We extracted the maximal exponential time constant (τ in Figure 4C), across limbs, for each species and observed a gradient across them (Figure 4D) with the smallest time constants observed in humans (0.035 ± 0.43), followed by mice (0.73 ± 0.2) and flies (1.89 ± 0.11). These results suggested that the timescale over which errors are corrected vary with many-legged embodiment – the correction timescale increased with the number of legs.

Thus, we found that the control magnitude and timescale for foot placement vary with many-legged embodiment; with larger number of limbs, the magnitude of the body state-dependent control decreased, and the control timescale became increasingly multi-step.

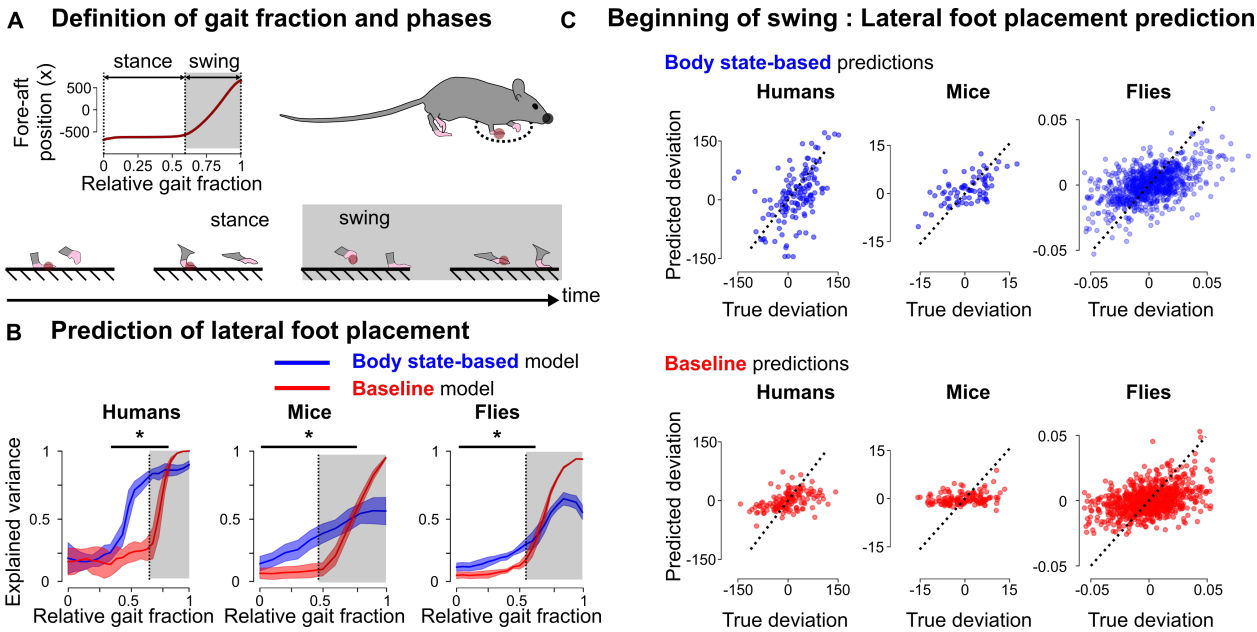

Figure 3: Signatures of body state-dependent feedback foot placement control. **A** We defined the gait fraction as the time elapsed since the last contact of the reference foot divided by the duration of the gait cycle. The stance and swing phase of each foot (here illustrated for the foot highlighted in red) were defined as the periods during which the foot was or was not in contact with the ground, illustrated here for one of the front limbs in mice. The swing-stance and stance-swing transitions correspond to contact initiation and contact termination. We built models to predict future contact initiation based on the kinematics of the body during the gait cycle preceding that contact. **B** Explained variance (R^2, median and interquartile range) obtained for the body state-based and baseline prediction models as a function of the relative gait fraction. The gray areas represent the swing phase of the foot to be placed, the vertical dashed lines represent the stance-swing transition for each species. **C** Comparison between the true and predicted deviations for the body state-based (top, blue) and baseline (bottom, red) predictions of the lateral foot placement of humans, mice and flies front limbs at the beginning of the swing phase of the contact foot (dashed line in panel **B**). The black dashed lines represent the identity lines corresponding to perfect prediction. $*p < 0.05$

Signatures of direction- and leg-specific modular control of foot placement

We have discovered shared signatures of body state-dependent foot placement control from locomotor variability in many-legged animals, and quantified how the control magnitude and timescale vary with embodiment. With the availability of multiple legs to execute the same functional goal, namely drift-free locomotion in the presence of sensorimotor errors, animals may use a more or less centralized control strategy i.e. they may use different legs or muscle groups for executing modular control functions. Here, we analyzed the locomotor variability to test the existence of such leg-specific or direction-specific modular control.

We hypothesized that, with the availability of multiple legs for control, medial and lateral errors i.e. errors that are directed towards and away from the body midline respectively, would be controlled differently (see Figure 5A). The rationale for this hypothesis is that medial errors are more likely to be corrected by the impedance of multiple stance legs in contact, compared to lateral errors. To test this hypothesis, we computed the feedback gains associated with medial and lateral body errors separately (see *Methods*) and compared them at the beginning of the swing phase of the foot being placed. Medial and lateral feedback gains were similar in humans (Figure 5B, left) but differed in mice (Figure 5B, center) and flies (Figure 5B, right), where the corrections were larger for lateral than for medial errors (Wilcoxon signed-rank, $p<0.05$ for both mice and flies). These results suggest the existence of error direction-dependent control of lateral foot placement in the front limbs of mice and flies. In simple words, the actions taken in response to lateral errors are larger than those taken in responses to medial errors in the body state.

Within a given embodiment, we posit that different pairs of limbs could have different control strategies; the rationale for this hypothesis is that in quadrupedal animals the front and hind limbs are innervated by different spinal circuits and therefore may exhibit distinct behavioral control signatures [25]. To test the existence of such leg-specific differences in control strategies, we compared the mapping between the body state errors and lateral foot placement between different

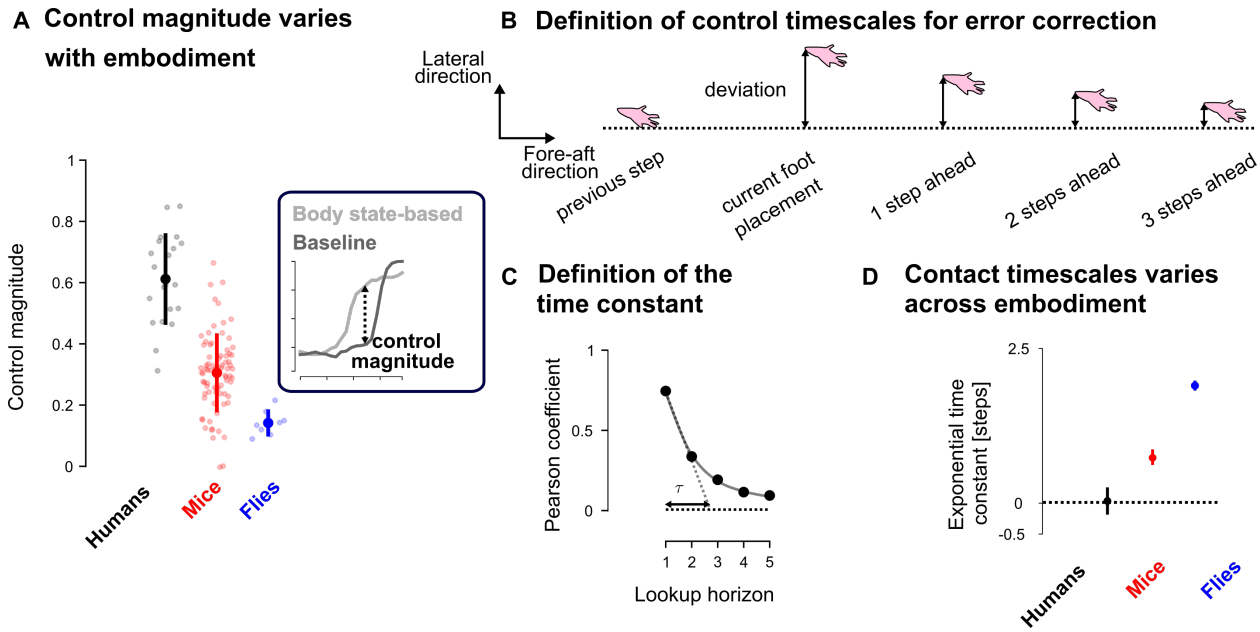

Figure 4: Control magnitude and timescale vary across embodiments. **A** Group median and interquartile range of the control magnitude for the lateral foot placements of humans legs (black), mice front legs (red) and flies front legs (blue) at the initiation of the swing phase of the contact foot. The control magnitude is defined as the difference between the amount of variance explained by the body state-based and the baseline prediction (see insert). **B** Schematic representation of the variations in the lateral foot placement as a function of time. We computed the correlation between the current lateral foot placement and the subsequent lateral foot placements. The Pearson coefficient of correlations exponentially decayed with the look up horizon as schematized in panel **C**. We characterized this exponential decay by the exponential time constant, τ. **D** Exponential time constants in humans, mice and flies (maximum across legs for each species). The error bar represent the centered 90% confidence interval based on bootstrap resampling.

pairs of limbs – from anterior to posterior as defined by the movement direction – over multiple gait cycles (Figure 5C). We observed that the correlations over a single gait cycle (see dashed inserts in Figure 5C) varied across legs; larger values were observed for more posterior limbs in both mice (Figure 5D red, Wilcoxon signed-rank test, $p<0.05$) and flies (Figure 5D blue, Kruskal-Wallis with posthoc Dunn's test and Bonferroni corrections, $p<0.05$). The exponential time constant associated with the decay of these correlations also varied across limbs in flies where the hind limbs had a smaller constant, i.e. a slower correction timescale, than the central limbs (Figure 5E). These results suggest that the control strategies for lateral foot placement in different limbs of flies and mice operate with different timescales – the more posterior pairs of limbs operate at slower timescales and have persistent control across multiple contacts.

Thus, we found that the control strategies used for foot placement by many-legged species reveal direction- and leg-specific modular control, exhibiting variation with error direction along the medial-lateral axis, and with limb pairs along the anterior-posterior axis relative to movement direction. We find that both the control gains and timescales exhibit such leg- and direction-specific modularity.

Discussion

We put forth a unified feedforward-feedback control structure underlying foot placement for stable locomotion in any legged animal. Based on this control structure, we developed a data-driven framework to discover signatures of control from natural locomotor variability across species. Using this framework, we discovered signatures of body state-dependent locomotor control in flies and mice, previously only shown to exist in humans. We found that the urgency of foot placement control, reflected in the control magnitude and timescale, decreased in more passively stable embodiment. Foot placement control was executed modularly in many-legged animals with the use of limb- and direction-specific gains and timescales. These findings have implications for understanding the neuromechanics of animal locomotion, uncovering the neural basis of stabilizing control, developing cross-species phenotypes for locomotor control, and bio-inspired legged robots.

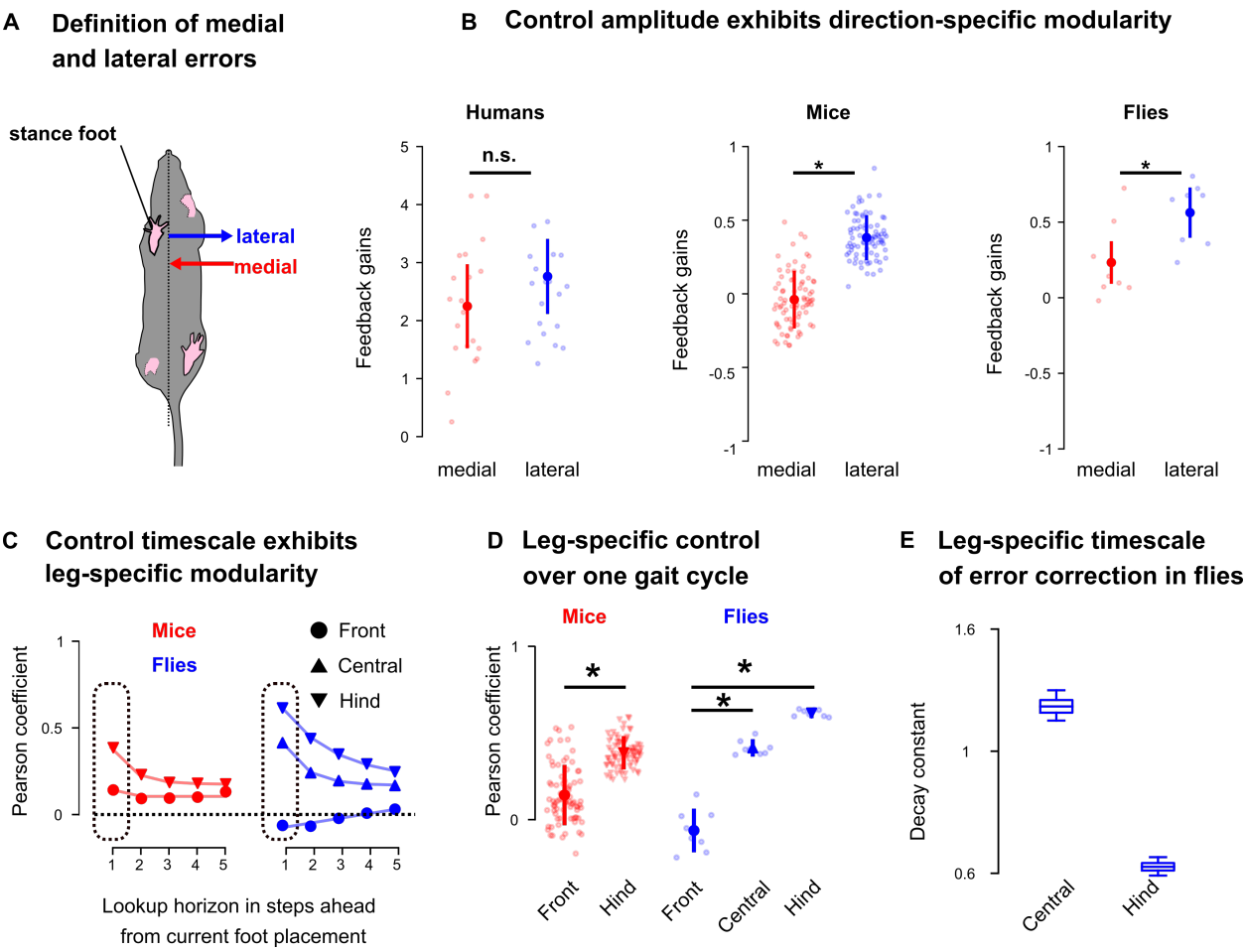

Figure 5: Foot placement control strategy reveals direction-specific and limb-specific modularity across species. **A** We illustrate the definition of lateral (blue) and medial (red) errors respectively as the errors directed away and towards the stance foot. We independently fitted predictive models for lateral and medial errors and compared their foot placement control gains. **B** Group median and interquartile range of the lateral (blue) and medial (red) foot placement control gains for humans, mice and flies at the beginning of the swing phase of the contact foot. **C** Pearson correlation coefficients as a function of lookup horizon for the different limbs in mice (left, red) and flies (right, blue), group median. **D** Group median and interquartile range of the initial Pearson correlation coefficient (see dashed rectangle in panel C) for the different pairs of limbs in mice and flies. **E** Timescale of the error corrections for central and hind limb in flies, the error bars capture the 90% confidence interval. $*p < 0.05$

We discovered signatures of body state-dependent control from unperturbed locomotor variability in many-legged animals, previously only shown to exist in humans [74, 89, 13]. Previous studies have investigated the dynamic stability of the average gait pattern adopted by an animal as a function of locomotion speed [85, 28]. These studies correspond to our feedforward velocity-dependent control module (Figure 1A, red), and do not provide evidence for body state-dependent control. Other works have characterized the fast timescale 'preflexive' lateral stabilization mechanisms in many-legged animals such as cockroaches [12, 49]. These preflexive mechanisms correspond to corrections made within the stance phase, and therefore are distinct from the slower multi-step swing foot control we discovered here (Figure 4). A few studies have shown the need for active control of lateral stabilization in many-legged animals for navigational control [21] and during perturbed locomotion [51], albeit without a unified feedforward-feedback account of control. In humans, there is some generalization of foot placement control from perturbed to unperturbed settings [80, 50]. Future work in animal locomotion can utilize our data-driven framework to separate body state-dependent contributions to stability from velocity-dependent contributions and can investigate whether unperturbed foot placement control is generalized to perturbed contexts.

The signatures of foot placement control we discover could help investigate the neural basis of stable locomotion, and its evolution across species. The differences we find between the velocity-dependent and the body state-dependent foot placement control (Figure 2, Figure 3) suggest that they have distinct but interacting underlying mechanisms. The fore-aft velocity-dependent foot placement is likely controlled by autonomous spinal circuits [18, 25] or by descending networks that control gait coordination [11]. The lateral body state-dependent foot placement (Figure 3B) provides evidence for an unconfirmed neural mechanism underlying feedback control during unperturbed animal locomotion. We propose that a candidate neural mechanism could be sensory feedback-guided steering, which has been found in mice [77], flies [30], and humans [22, 10], but has not been shown to underlie stabilizing control. This candidate neural mechanism is plausible given that the feedback signatures we discovered occured at timescales longer than the sensorimotor delays inherent to these species [61]. We discover that foot placement control depends on phase-locked error information, which could be obtained neurally by using an efference copy from pattern generating circuits to filter the feedforward contributions to sensory information [37]. The mechanism underlying the observed foot placement control may also involve the cerebellum in mammals or the central complex in insects to combine desired nominal sensory states with multimodal feedback in order to estimate the error to be corrected [4, 70, 56, 30, 71, 78, 88, 36]. We discovered signatures of error direction-dependent control of foot placement with different gains for medial and lateral errors (Figure 5). Future studies can identify where in the neural control hierarchy this error direction-selectivity is established: the spine [18], the cerebellum [79], or the vestibular region [92] to better understand the neural basis of centralization across species [66]. Thus, future work can utilize our conceptual and data-driven foot placement control framework to identify the neural mechanisms underlying the observed control signatures.

Our framework can be generalized to a number of legged species with diverse center of mass height, number of legs, and passive limb impedance to understand how such biomechanical embodiment co-evolved with the nervous systems to achieve foot placement control. We found significant variations in both the control amplitude and timescale with more passively stable many-legged embodiment. These differences highlight the importance of biomechanical embodiment to the neural control of locomotion [68, 86], and allow the cross-species differences in control to be quantifiably compared. Our framework can be used in combination with imitation learning to align simulations of embodied control in different species with natural locomotor variability [90, 60]. These findings can also inform the development of bio-inspired cross-embodiment control [95] in many-legged robots, for instance, by providing bio-inspiration for the selection of locomotor control primitives (Figure 5). Understanding how locomotor control strategies vary with neuromechanical embodiment for a shared functional goal can elucidate the principles underlying the co-evolution of biomechanics and control.

By identifying signatures of control hidden in natural variability in flies, mice, and humans, our work provides a way to compare control strategies across species for a shared ethological goal: foot placement control. Investigating animal locomotion in such an ethological setting has some limitations. One key limitation is the inability to know, from behavior alone, the precise nature of the noise-like input to the controller which results in errors to be controlled. Here, we hypothesized that the observed variability is the result of feedforward-feedback control in response intrinsic sensorimotor noise (Figure 1A), which has some theoretical validity [39, 80], but confirming whether this noise is motor, sensory, or neural in origin is challenging with theory and behavior alone [65]. This challenge can be an opportunity for future neuroscience research to uncover the noisy input that results in errors during unperturbed locomotion. Another limitation of studying locomotor control strategies from natural variability is the lack of control afforded to the experimenter compared to settings where external perturbations are applied to the animal. However, these two approaches need not be mutually exclusive; in human locomotion, studying foot placement control both in the presence and absence of external perturbations has proven fruitful [80, 50].

There are also advantages to studying the control strategies underlying natural variability, such as the ecological validity of the control principles discovered, the relevance to easily quantifiable clinical biomarkers, and the ease of reproducibility. Understanding the control strategies that enable stable locomotion in ecologically valid settings, as we have done here, can help discover the underlying neural principles, and is aligned with the current push towards neuroscience in ethological settings [23, 26, 17]. Population differences in human locomotor variability are used as biomarkers for neuromotor disorders that impair balance, such as Parkinson's disease [63]. Here, we have shown that neuroscientifically accessible animals models like flies and mice exhibit human-like signatures of control hidden in variability, thus encouraging the study of these control signatures as potential cross-species biomarkers in healthy and impaired animal models. Our approach is easily reproducible as it is applicable to any many-legged animal (see *Methods*), builds on open source video processing pipelines [58, 69], and does not require specialized equipment other than a camera placed such that foot contacts are discernible. Moreover, as locomotion is a naturalistic behavior that is readily exhibited by many animals, our framework can enable post-hoc analyses of large-scale observational animal behavior datasets [53].

Methods

Mathematical formulation of feedforward-feedback foot placement control

We hypothesize that foot placement control in any many-legged animal is generated by a feedforward-feedback control structure (Figure 1A) composed of a velocity-dependent feedforward module and a body state-dependent feedback module. This control structure outputs the net observed foot placement as the resultant of the contribution of its two control modules (Figure 1D): the feedforward module contributes the foot placement prescribed by the canonical gait patterns [35] while the feedback module contributes body state error-based corrective adjustments of foot placement [89]. These modules operate at different timescales and are organized in a *hierarchical* manner such that each of them has access to some privileged information which is not available to the other. The input to the feedforward control module is the average velocity during the last gait cycle $\hat{v}$ while the inputs to the feedback control module are the body state deviations from the stereotypical species-specific gait pattern Q^*, expressed as phase-dependent body state-errors $\Delta Q(\phi) = Q(\phi) - Q^*(\phi)$, where ϕ is the relative gait fraction defined as the ratio between the duration since the beginning of the last gait cycle and the total duration of that gait cycle. For each step, the net observed foot placement was expressed as the sum of the individual contributions from the two control modules

$$P = f\left(\hat{v}\right) + g\left(\Delta Q\left(\phi\right)\right), \tag{1}$$

where functions f and g are respectively the contributions of the feedforward and feedback control modules. We used the data from naturalistic locomotion of different legged species to investigate signatures of the hypothesized control structure across species.

Inference of control signatures from locomotion data

We combined the hypothesized control structure underlying legged locomotion with a data-driven framework to investigate signatures of feedforward and feedback foot placement control. First, we investigated the velocity-dependent component of foot placement in the fore-aft and lateral directions. To do this, we generalized the methodology used in humans to many-legged embodiment [19]: for each gait cycle, we defined the movement velocity as the average fore-aft velocity of the body during the last gait cycle. We observed that the relationships between the movement velocity and the fore-aft and lateral foot placement were linear (Figure 2B) and characterized this relationship with the model

$$f_j^{x,y}\left(\hat{v}\right) = \beta_{0,j}^{x,y} + \beta_{1,j}^{x,y}\hat{v}, \tag{2}$$

where $\beta_{0,j}^{x,y}$ and $\beta_{1,j}^{x,y}$ are scalar model parameters capturing the relationships for the jth leg along the fore-aft (x) and lateral (y) direction. We used individual models for each animal subject and for each limb to capture how that limb's step length and width were modulated by the average velocity.

To investigate the behavioral control signatures of the hypothesized feedback module, we defined the body state errors as the difference between the body state kinematics (positions and velocities) during the last gait cycle $Q\left(\phi\right)$ and the velocity-dependent body states as specified by the stereotypical gait pattern $\Delta Q(\phi) = Q(\phi) - Q^*_{\hat{v}}(\phi)$, where $\hat{v}$ is the average velocity over that gait cycle. We defined the corrective foot placements as the difference between the net observed foot placement P and the ones predicted by the feedforward control module $\Delta P = P - f^{x,y}\left(\hat{v}\right)$. We observed linear relationships between the body state errors and the corrective foot placements (Figure 3B), which is theoretically valid for small errors, because continuous and differentiable nonlinear functions can be approximated as linear for infinitesimal changes. We investigated these relationships for the jth leg by the model

$$\Delta P \approx g_j^{x,y}\left(\Delta Q\left(\phi\right)\right) = \gamma_{0,j}^{x,y} + \sum_{i=1}^{N} \gamma_{i,j}^{x,y} \Delta Q\left(\phi\right), \tag{3}$$

where $\gamma_{i,j}^{x,y}$ are scalar model parameters and N is the dimensionality of deviation vector.

We investigated the behavioral signatures of the feedback control module across species by comparing their amplitude and timescale. The control amplitudes were quantified as the maximal individual differences between the amount of variance explained by the body state-dependent feedback model (blue traces in Figure 3B) and that of a baseline model predicting the variability in foot placement from the foot kinematics itself (red traces in Figure 3B). This baseline model, expressed as a function of the deviations in body kinematics $\Delta\tilde{Q}(\phi) = \tilde{Q}(\phi) - \tilde{Q}^*(\phi)$, was formalized as

$$\Delta P \approx \tilde{g}_j^{x,y}\left(\Delta\tilde{Q}\left(\phi\right)\right) = \tilde{\gamma}_{0,j}^{x,y} + \sum_{i=1}^{N} \tilde{\gamma}_{i,j}^{x,y} \Delta\tilde{Q}\left(\phi\right). \tag{4}$$

We then investigated the control timescales by correlating successive lateral positions of each foot over multiples gait cycles. The limb-specificity of the feedback control module was investigated by separating the medial and lateral errors

and using the feedback model described above. Consistent with anatomical definitions, these direction-dependent errors $\Delta Q_{p_y}(\phi)$ are defined as follows: medial errors are directed towards the body while lateral are directed away from the body (Figure 5A.)

Datasets used to investigate foot placement control across species

The contributions of the feedforward and feedback control modules can be inferred for any dataset for which kinematics data of the body and feet are available. To demonstrate this flexibility, we chose to use existing open source datasets of flies, mice and humans during natural locomotion collected across different research groups.

The fly locomotion dataset was collected by DeAngelis and colleagues [24] with a Point Grey camera (Flea3-U3-13Y3M-C, 150Hz) when 8 groups of 12 to 15 flies (*Drosophila melanogaster*) were evolving in an open-field arena during 1.1h. The data was segmented into individual locomotion bouts and the body and feet positions, as well as the individual foot contacts were extracted by the original authors using a custom-built markerless motion capture method (see [24] for more details). We used the feet and the head markers in our analyses and only considered the segments during which the animals were not stopping. The mouse locomotion dataset was collected by Klibaite and colleagues [53] with a Point Grey greyscale camera (12-bit greyscale, 1280 x 1024 pixels, 80Hz) when mice (C57BL/6J) were moving in an open-field arena on 4 consecutive days, 20 minutes each day. The positions of the different body parts were extracted using LEAP [69], an open source markerless pose estimation software. We used the feet, nose, and base of the tail markers for our analyzes and only considered the data segments labeled as locomotion. The human locomotion dataset was collected by Camargo and colleagues [15] using 32 motion capture markers placed according to the Helen Hayes Hospital marker set (Vicon. Ltd, Oxford, UK). The data were collected at a frequency of 200Hz and was filtered using a 4th order zero-lag Butterworth filter (cutoff frequency 6Hz) during overground walking. We used the pelvis position, defined as the average position of the four hip markers, and the foot position, approximated by the position of the heel markers. We also used another human locomotion dataset collected by Wang and Srinivasan [89] for some analyzes, the data collection procedure was the same as that of the Camargo dataset and we used the same set of markers.

Processing pipeline for obtaining the inputs and outputs of the foot placement controller

In this section, we describe how we processed the raw data described above to transform them into the inputs and outputs to the feedforward and feedback control modules. We sought to use an identical processing pipeline for all the datasets. In line with this, the steps outlined below were applied to all the datasets and species, unless otherwise stated.

We were interested in studying the straight-line locomotion bouts since foot placement control has only been characterized during straight-line locomotion in previous theoretical and human literature [87, 43, 89]. We therefore selected the locomotion bouts for which the body orientation defined as the direction of the instantaneous velocity vector in the horizontal plane did not vary by more than 30 degrees. We then rotated these straight-line locomotion bouts to align the heading direction across bouts, since the raw data contained locomotion bouts that can have different orientations in the world coordinates. We next identified the timing of each foot contact to extract the contact locations and segmented the gait cycles. For the datasets in which the contact timings were not provided, we computed the distance between the feet and body markers in the horizontal plane and defined the beginning and end of the stance phases as the maxima and minima of that distance [5]. We defined the contact locations, $P = [p_x, p_y]^T$ as the average positions of the foot markers during their stance phases. We used the contact initiations i.e. the beginning of the stance phases to perform the gait segmentation, defining a gait cycle as the interval between two successive contact initiations of a same leg. We performed this gait segmentation independently for each limb and grouped the gait cycles associated with the same limb.

Because the inputs to the feedback control module are posited to be phase-dependent $\Delta Q(\phi)$, we temporally normalized the segmented gait cycles by linearly interpolating their marker positions and velocities onto a fixed set of discrete phases ϕ. The number of phases for each species was set to the average number of frames per gait cycle in the raw data. Thus, body and foot states are represented relative to phase ϕ, with $\phi = 0$ corresponding to the beginning of the gait cycle and $\phi = 1$ to the end of the gait cycle, which is when the contact corresponding to foot placement occurs. We then spatially normalized the marker positions and the contact locations by subtracting the last contact location of the front limb belonging to the opposite group of limbs. We defined the opposite group of limbs based on the canonical gait patterns whereby two groups of limbs are moving in opposite phase during walking (filled and empty rectangles in Figure 1B).

Statistical analyses

We characterized the impact of movement velocity on the step length and width by fitting individual linear regressions. We used the function SCIPY.STATS.LINREGRESS in Python to fit these regressions and kept track of the individual slopes and p values associated with each of these.

To infer the feedback control module, we obtained linear models between the body errors $\Delta Q(\phi)$ and the foot placement deviations ΔP (see above for more details). The best fit model parameters, obtained by the minimization of the mean squared errors, were given by $\hat{K}(t) = \frac{\Delta Q(\phi)^T \Delta P}{\Delta Q(\phi)^T \Delta Q(\phi)}$ and the coefficient of determinations were given by $R^2 = 1 - \frac{\Sigma r^2}{\Sigma \Delta P^2}$, where $r = \Delta \hat{P} - \Delta P$ are the residual errors associated with the multiple linear regression.

To investigate whether errors were corrected over multiple gait cycles, we investigated the correlations between successive lateral foot placements for each leg. We computed these correlations between lateral foot placements at time t and those at time $t + N$ where N is an integer value capturing the lookup horizon. We then obtained the exponential decay capturing the variation of the Pearson coefficient with the lookup horizon. We used bootstrap resampling (n=10 000) to evaluate the parameters of this exponential decay and reported the 90% confidence interval for each of the parameters we studied.

We used non-parametric versions of all the statistical tests we performed. We used the two-samples Kolmogorov-Smirnov test to compare distributions, the Wilcoxon-ranked test to compare medians, and the Kruskal-Wallis test with Dunn's posthoc tests to compare medians of more than two groups. The p values resulting from multiple comparisons were adjusted using the Bonferroni correction. We reported significance when the p value fell below 0.05.

Acknowledgments

Antoine De Comite is supported by a postdoctoral fellowship of the K. Lisa Yang Integrative Computational Neuroscience (ICoN) Center at MIT.

References

[1] T Akay and A J Murray. Relative contribution of proprioceptive and vestibular sensory systems to locomotion: Opportunities for discovery in the age of molecular science. *International Journal of Molecular Sciences*, 22:1467, 2021.

[2] D E Angelaki and K E Cullen. Vestibular system : The many facets of a multimodal sense. *Annual Reviews in Neuroscience*, 31:125–150, 2008.

[3] E Anson, P Agada, T Kiemel, Y Ivanenko, F Lacquaniti, and J Jeka. Visual control of trunk translation and orientation during locomotion. *Experimental Brain Research*, 232:1941–1951, 2013.

[4] Y I Arshavsky, M B Berkinblit, O I Fukson, I M Gelfand, and G N Orlovsky. Origin of modulation in neurones of the ventral spinocerebellar tract during locomotion. *Brain Research*, 43:276–279, 1972.

[5] J J Banks, W-R Chang, X Xu, and C-C Chang. Using horizontal heel displacement to identify heel strike in normal gait. *Gait and Posture*, 42:101–103, 2015.

[6] C E Bauby and A D Kuo. Active control of lateral balance in human walking. *Journal of Biomechanics*, 33:1433–1440, 2000.

[7] C Bellardita and O Kiehn. Phenotypic characterization of speed-associated gait changes in mice reveals modular organization of locomotor networks. *Current Biology*, 25:1426–1436, 2015.

[8] L R Bent, T I Inglis, and B J McFadyen. When is vestibular information important during walking ? *Journal of Neurophysiology*, 92:1269–1275, 2004.

[9] J E Bertram and A Ruina. Multiple walking speed-frequency relations are predicted by constrained optimization. *Journal of theoretical Biology*, 209:445–453, 2001.

[10] M Bove, G Courtine, and M Schieppati. Neck muscle vibration and spatial orientation during stepping in place in humans. *Journal of Neurophysiology*, 88:2232–2241, 2001.

[11] Jonas Braun, Femke Hurtak, Sibo Wang-Chen, and Pavan Ramdya. Descending networks transform command signals into population motor control. *Nature*, pages 1–9, 2024.

[12] I E Brown and G E Loeb. *A reductionnist approach to creating and using neuromusculoskeletal models*. Springer New York, 2000.

[13] S M Bruijn and J H van Dieën. Control of human gait stability through foot placement. *Journal of the Royal Society Interface*, 15, 2018.

[14] V Caggiano, R Leiras, H Goñi-Erro, D Masini, C Bellardita, J Bouvier, V Caldeira, G Fisone, and O Kiehn. Midbrain circuits that set locomotor speed and gait selection. *Nature*, 553:455–460, 2018.

[15] J Camargo, A Ramanathan, W Flanagan, and A Young. A comprehensive, open-source dataset of lower limb biomechanics in multiple conditions of stairs, ramps, and level-ground ambulation and transitions. *Journal of Biomechanics*, 112:110320, 2021.

[16] C Chun, T Biswas, and V Bhandawat. Drosophila uses a tripod gait across all walking speed, and the geometry of the tripod is important for speed control. *eLife*, page e65878, 2021.

[17] P Cisek and A M Green. Towards a neuroscience of natural behavior. *Current opinion in Neurobiology*, 86, 2024.

[18] J J Collins and I N Stewart. Coupled nonlinear oscillators and the symmetry of animal gaits. *Journal of Nonlinear Science*, 3:349–392, 1993.

[19] S H Collins and A D Kuo. Two independent contributions to step variability during over-ground human walking. *PloS One*, 8:e73597, 2013.

[20] G Courtine, A M De Nunzio, M Schmid, Berettan M V, and M Schieppati. Stance- and locomotion-dependent processing of vibration-induced proprioceptive inflow from multiple muscles in humans. *Journal of Neurophysiology*, 97:772–779, 2007.

[21] N J Cowan, J Lee, and R J Full. Task-level control of rapid wall following in the american cockroach. *Journal of Experimental Biology*, 209:1617–1629, 209.

[22] C J Dakin, J T Inglis, R Chua, and J-S Blouin. Muscle-specific modulation of vestibular reflexes with increased locomotor velocity and cadence. *Journal of neurophysiology*, 110(1):86–94, 2013.

[23] S R Datta, D J Anderson, K Branson, P Perona, and A Leifer. Computational neuroethology: a call to action. *Neuron*, 104(1):11–24, 2019.

[24] B D DeAngelis, J A Zavatone-Veth, and D A Clark. The manifold structure of limb coordination in walking drosophila. *eLife*, page e46409, 2019.

[25] F Delcomyn. Neural basis of rhythmic behavior in animals. *Science*, 210:492–498, 1980.

[26] E J Dennis, A El Hady, A Michail, A Clemens, D R Gowan Tervo, J Voigts, and S R Datta. Systems neuroscience of natural behavior in rodents. *Journal of Neuroscience*, 41:911–919, 2021.

[27] M H Dickinson, C T Farley, R J Full, M A R Koehl, R Kram, and S Lehman. How animals move : An integrative view. *Science*, 288:100–106, 2000.

[28] B J Farrel, M A Bulgakova, I N Beloozerova, M G Sirota, and B I Prilutsky. Body stability and muscle and motor cortex activity during walking with wide stance. *Journal of Neurophysiology*, 112:502–504, 2014.

[29] R C Fitzpatrick, D L Wardman, and J L Taylor. Effects of galvanic vestibular stimulation during human walking. *Journal of Physiology*, 517:931–939, 1999.

[30] T Fujiwara, M Brotas, and M E Chiappe. Walking strides direct rapid and flexible recruitment of visual circuits for course control in drosophila. *Neuron*, 110:2124–2138, 2022.

[31] Pearson K G. Common principles of motor control in vertebrates and invertebrates. *Annu. Rev. Neurosci*, 16:265–297, 1993.

[32] R Gal and F Libersat. New vistas on the initiation and maintenance of the insect motor behaviors revealed by specific lesions of the head ganglia. *Journal of Comparative Physiology A*, 192:1003–1020, 2006.

[33] T Garland. The relation between maximal running speed and body mass in terrestrial animals. *Journal of Zoology*, 199:157–170, 1983.

[34] Y Gerasimenko, R R Roy, and V R Edgerton. Epidural stimulation: Comparison of the spinal circuits that generate and control locomotion in rats, cats and humans. *Experimental Neurology*, 209:417–425, 2008.

[35] A I Goncalves, J A Zavatone-Veth, M R Carey, and D A Clark. Parallel locomotor control strategies in mice and flies. *Current Opinion in Neurobiology*, 73, 2022.

[36] J Green, A Adachi, K K Shah, J D Hirokawa, P S Magani, and G Maimon. A neural circuit architecture for angular integration in drosophila. *Nature*, 546:101–106, 2017.

[37] S Grillner and A El Manira. Current principles of motor control, with a special reference to vertebrate locomotion. *Physiological Reviews*, 100:271–320, 2019.

[38] D Hamacher, F Herold, P Wiegel, D Hamacher, and L Schegga. Brain activity during walking: A systematic review. *Neuroscience and Biobehavioral Reviews*, 57:310–327, 2015.

[39] Christopher M Harris and Daniel M Wolpert. Signal-dependent noise determines motor planning. *Nature*, 394(6695):780–784, 1998.

[40] N C Heglund, C R Taylor, and T A McMahon. Scaling stride frequency and gait to animal size : mice to horses. *Science*, 186:1112–1113, 1974.

[41] M Hildebrand. Symmetrical gaits of horses. *Science*, 150:701–708, 1965.

[42] M Hildebrand. The quadrupedal gaits of vertebrates. *Bioscience*, 39, 1989.

[43] A L Hof, M G J Gazendam, and W E Sinke. The condition for dynamic stability. *Journal of Biomechanics*, 38(1):1–8, 2005.

[44] C P Hurt, N Rosenblatt, J R Crenshaw, and M D Grabiner. Variation in trunk kinematics influences the variation in step width during treadmill walking by older and younger adults. *Gait and Posture*, 31:461–464, 2010.

[45] J R Hutchinson. The evolutionary biomechanics of locomotor function in giant land animals. *Journal of Experimental Biology*, 224, 2021.

[46] A J Iijspeert and M A Daley. Integration of feedforward and feedback control in the neuromechanics of vertebrate locomotion: a review of experimental, simulations and robotic studies. *Journal of Experimental Biology*, 226:jeb245784, 2023.

[47] A J Ijspeert. Central pattern generators for locomotion control in animals and robots: A review. *Neural networks*, 21:642–653, 2008.

[48] W Ilg, H Golla, P Thier, and M A Giese. Specific influences of cerebellar dysfunctions on gait. *Brain*, 130:786–798, 2007.

[49] D L Jindrich and R J Full. Dynamic stabilization of rapid hexapedal locomotion. *Journal of Experimental Biology*, 205:2803–2823, 2002.

[50] V Joshi and M Srinivasan. A controller for walking derived from how humans recover from perturbations. *Journal of The Royal Society Interface*, 16(157):20190027, 2019.

[51] A Karayannidou, I N Beloozevora, P V Zelenin, E E Stout, M G Sirota, G N Orlovsky, and T G Deliagina. Activity of pyramidal tract neurons in the cat during standing and walking on an inclined plane. *Journal of Physiology*, 587:3795–3811, 2009.

[52] D Kindregan, L Gallagher, and J Gromley. Gait deviations in children with autism spectrum disorders: A review. *Autism Research and Treatment*, 2015, 2015.

[53] U Klibaite, M Kislin, J L Verpeut, S Bergeler, X Sun, J Z Shaevitz, and S S-H Wang. Deep phenotyping reveals movement phenotypes in mouse neurodevelopmental models. *Molecular Autism*, 13:12, 2022.

[54] A D Kuo. The relative roles of feedforward and feedback in the control of rhythmic movements. *Motor Control*, 6:129–145, 2002.

[55] D Labonte, P J Bishop, T J M Dick, and C J Clemente. Dynamic similarity and the peculiar allometry of maximum running speed. *Nature Communications*, 15, 2024.

[56] A Mamiya, P Gurung, and J C Tuthill. Neural coding of leg proprioception in drosophila. *Neuron*, 100:636–650, 2018.

[57] C Mantziaris, T Bockemuhl, and A Buschges. Central pattern generating networks in insect locomotion. *Developmental Neurobiology*, 80:16–30, 2020.

[58] A Mathis, P Mamidanna, K M Cury, Abe T, V N Murthy, M W Mathis, and M Bethge. Deeplabcut: markerless pose estimation for user-defined body parts. *Nature Neuroscience*, 21:1281–1289, 2018.

[59] P M McAndrew, J B Dingwell, and J M Wilken. Walking variability during continuous pseudo-random oscillations of the support surface and visual field. *Journal of Biomechanics*, 43:1470–1475, 2010.

[60] J Merel, D Aldarondo, J Marshall, Y Tassa, G Wayne, and B Ölveczky. Deep neuroethology of a virtual rodent. *aRxiv*, 2019.

[61] H L More and J M Donelan. Scaling of sensorimotor delays in terrestrial mammals. *Proceedings of the Royal Society B*, 285:20180613, 2018.

[62] H L More, J R Hutchinson, D F Collins, D J Weber, S K H Aung, and J M Donelan. Scaling of sensorimotor control in terrestrial mammals. *Proceedings of the Royal Society B: Biological Sciences*, 277:3563–3568, 2010.

[63] M E Morris, F Huxham, J McGinley, K Dodd, and R Iansek. The biomechanics and motor control of gait in parkinson disease. *Clinical Biomechanics*, 16:459–470, 2001.

[64] S M Morton and A J Bastian. Mechanisms of cerebellar gait ataxia. *The Cerebellum*, 6:79–86, 2007.

[65] A Nagamori, C M Laine, G E Loeb, and F J Valero-Cuevas. Force variability is mostly not motor noise: Theoretical implications for motor control. *PLoS Computational Biology*, 17(3):e1008707, 2021.

[66] I D Neveln, A Tirumalai, and S Sponberg. Information-based centralization of locomotion in animals and robots. *Nature Communications*, 10:3655, 2019.

[67] J A Nirodi. Universal features in panarthropod inter-limb coordinatino during forward walking. *Integrative and Comparative Biology*, 61:710–722, 2021.

[68] K Nishikawa, A A Biewener, P Aerts, A N Ahn, H J Chiel, M A Daley, T L Daniel, R J Full, M H Hale, T L Hedrick, A K Lappin, T R Nichols, R D Quinn, R A Satterlie, and B Szymik. Neuromechanics: An integrative approach for understanding motor control. *Integrative and Comparative Biology*, 47:16–54, 2007.

[69] T D Pereira, D E Aldarondo, L Willmore, M Kislin, S S-H Wang, M Murty, and J W Shaevitz. Fast animal pose estimation using deep neural networks. *Nature Methods*, 16:117–125, 2019.

[70] K Pfeiffer and U Homberg. Organization and functional roles of the central complex in the insect brain. *Annual Review of Entomology*, 59:165–184, 2014.

[71] B G Pratt, S-Y G Lee, G M Chou, and J C Tuthill. Miniature linear and split-belt treadmills reveal mechanisms of adaptive motor control in walking drosophila. *bioRxiv*, 2024.

[72] M H Raibert. Hopping in legged systems—modeling and simulation for the two-dimensional one-legged case. *IEEE Transactions on Systems, Man, and Cybernetics*, 3:451–463, 1984.

[73] M H Raibert, H B Brown, M Chepponis, and E Hastings. Dynamically stable legged locomotion research: December 1, 1980-september 30, 1981. Technical report, Carnegie Mellon University, 1981.

[74] B L Rankin, S K Buffo, and J C Dean. A neuromechanical strategy for mediolateral foot placement in walking humans. *Journal of Neurophysiology*, 112(2):374–383, 2014.

[75] D C Roden-Reynolds, M H Walker, C R Wasserman, and J C Dean. Hip proprioceptive feedback influences the control of mediolateral stability during human walking. *Journal of Neurophysiology*, 114:2220–2229, 2015.

[76] S Rossignol, R Dubuc, and J-P Gossard. Dynamic sensorimotor interactions in locomotion. *Physiological Reviews*, 86:89–154, 2006.

[77] L Ruder, A Takeoka, and S Arber. Long-distance spinal neurons ensure quadrupedal locomotor stability. *Neuron*, 92:1063–1078, 2016.

[78] A Santuz, T Akay, W P Mayer, T L Wells, A Schroll, and A Arampatzis. Modular organization of murine locomotor pattern in the presence and absence of sensory feedback from muscle spindles. *The Journal of Physiology*, 597:3147–3165, 2019.

[79] B A Sauerbrei, E V Lubenov, and A G Siapas. Structured variability in purkinje cell activity during locomotion. *Neuron*, 87:840–852, 2015.

[80] N Seethapathi and M Srinivasan. Step-to-step variations in human running reveal how humans run without falling. *eLife*, page e38371, 2019.

[81] J Seipel and P Holmes. Three-dimensional translational dynamics and stability of multi-legged runners. *The International Journal of Robotics Research*, 25:889–902, 2006.

[82] M Shafiee, G Bellegarda, and A Ijspeert. Manyquadrupeds: Learning a single locomotion policy for diverse quadruped robots. *International Conference of Robotics and Automation*, 2024.

[83] H Shimada, K Ishii, K Ishiwata, K Oda, M Suzukawa, H Makizako, T Doi, and T Suzuki. Gait adaptability and brain activity during unacustomed treadmill walking in healthy elderly females. *Gait and Posture*, 38:203–208, 2013.

[84] S N M Thangal and J M Donelan. Scaling of inertial delays in terrestrial animals. *Plos One*, 15, 2020.

[85] L H Ting, R Blickhan, and R J Full. Dynamic and static stability in hexapedal runners. *Journal of Experimental Biology*, 197:251–269, 1994.

[86] L H Ting, H J Chiel, R D Trumbower, J L Allen, J L McKay, M E Hackney, and T M Kesar. Neuromechanical principles underlying movement modularity and their implications for rehabilitation. *Neuron*, 86:38–54, 2015.

[87] M A Townsend. Biped gait stabilization via foot placement. *Journal of Biomechanics*, 18(1):21–38, 1985.

[88] P-P Vidal, L Degallaix, P Josset, J-P Gasc, and K E Cullen. Postural and locomotor control in normal and vestibular deficient mice. *The Journal of Physiology*, 559:625–638, 2004.

[89] Y Wang and M Srinivasan. Stepping in the direction of the fall: the next foot placement can be predicted from current upper body state in steady-state walking. *Biology Letters*, 10, 2014.

[90] S Wang-Chen, V A Stimpfling, P G Özdil, L Genoud, F Hurtak, and P Ramdya. Neuromechfly 2.0, a framework for simulating embodied sensorimotor control in adult drosophila. *bioRxiv*, 2023.

[91] K E Webster, J R Merory, and J E Wittwer. Gait variability in community dwelling adults with alzheimer disease. *Alzheimer Disease and Associated Disorders*, 20:37–40, 2006.

[92] E C Witts and A J Murray. Vestibulospinal contributions to mammalian locomotion. *Current Opinion in Physiology*, 8:56–62, 2019.

[93] H H Yang, L E Brezovec, L S Capdevilla, Q X Vanderbeck, A Adachi, R S Mann, and R I Wilson. Fine-grained descending control of steering in walking drosophila. *bioRxiv*, 2023.

[94] R Zacarias, S Namiki, G M Card, M L Vasconcelos, and A M Moita. Speed dependent descending control of freezing behavior in drosophila melanogaster. *Nature Communications*, 8:3697, 2018.

[95] K Zakka, A Zeng, P Florence, J Tompson, J Bohg, and D Dwibedi. Xirl: Cross-embodiment inverse reinforcement learning. *CORL*, 2021.